DOI: 10.53469/jpce.2026.08(01).07

Study on Creep Characteristics of Soft Rock in the Foundation of a Power Plant

Haoqin Mei, Ziwang Yu*, Chuanxiang Zhang, Xu Guo

College of Construction Engineering, Jilin University, Changchun 130021, Jilin, China
Correspondence Author

Abstract: ***Soft rock exhibits prominent creep characteristics in foundation engineering, which are prone to induce deformation and instability of engineering structures. Taking the soft rock in the foundation of a power plant as the research object, this paper systematically analyzes the creep mechanical behavior of soft rock through field in-situ load tests and laboratory uniaxial compression tests. Based on the Burgers creep model, the creep parameters under different load levels are obtained via fitting, and the characteristics of instantaneous elasticity, decelerated creep and steady-state creep of soft rock are discussed. The research results can provide a theoretical basis for the evaluation and design of long-term foundation stability in similar engineering projects.***

Keywords: Soft rock, Creep characteristics, Burgers model, In-situ test, Parameter identification.

1. Introduction

Rock creep models are an important component of theoretical research on rock rheological mechanics, and also one of the difficulties and hotspots in current rock mechanics research [1] [2]. A qualified rock creep model is required to not only accurately reflect the creep characteristics of rocks, but also take into account the feasibility and certain universality of practical engineering applications. One of the core contents of rock creep characteristic research is the establishment and application of creep models [3]. After years of research, the theory of rock creep models has achieved substantial development, and a large number of creep models have been proposed. For different types of rocks, corresponding creep models can be selected to describe their characteristics. According to existing research, creep models in rock mechanics can be roughly divided into three categories, namely empirical formulas, composite models (physical models), and integral models (mathematical models), all of which have been widely applied in engineering practice [4]. The future development trend is to study and establish nonlinear creep models, and determine various creep parameters of rock masses based on triaxial creep tests [5] [6].

Soft rocks with obvious creep characteristics are frequently encountered in underground construction projects, such as uncemented sandstone, mudstone, sandy mudstone, and clay shale [7] [8]. This type of rock mass exhibits large creep deformation, manifesting as severe extrusion deformation from all directions of underground engineering, which often leads to the instability and failure of support structures or foundation systems [9]. A large number of engineering practices have shown that excessive harmful deformation is the main cause of instability in underground engineering excavated in such rock masses [10]. Taking the soft rock in the foundation of a power plant as the research object, this paper conducts in-situ load tests and laboratory tests, obtains a large amount of test data, investigates the creep laws of soft rock, and establishes a creep constitutive model suitable for the specific geological conditions, so as to provide a scientific basis for the long-term stability of the engineering project [11] [12] [13].

2. Engineering Geological Conditions

The test site of this study is located at the top of a hill on the edge of a factory area. The surface is mainly covered by a 2–4 m thick layer of Upper Pleistocene alluvial-proluvial deposits of the Quaternary System, with lithology consisting of grayish-yellow, yellowish-brown and brick-red silty clay. Underlying the silty clay is the Tertiary sandstone, which is classified as weakly cemented and poorly consolidated semi-rock due to the low cementation degree between particles. It represents a transitional type between soil and rock, with argillaceous or calcareous cementation. The Tertiary sandstone has relatively low mechanical strength, which decreases significantly especially when it is saturated with water. The target site for field tests is shown in Figure 1.

Figure 1: Layout of the Target Site for Field Tests

The selection of the field test site was comprehensively determined by considering factors such as the thickness of overlying strata in the factory area and transportation conditions. The strata in the site are mainly composed of incompletely lithified Tertiary formations, with lithology including brownish-red and purplish-red medium-coarse grained sandstone, silty-fine sandstone and mudstone. These rocks contain a high content of mica flakes and clay minerals. Based on the preliminary drilling data and combined with the

stratigraphic column information, the burial depth of the target stratum was determined. On the basis of selecting sampling points, the field test site was finalized by synthetically evaluating geological conditions, stratigraphic information, thickness of overlying strata in the factory area, site scale and transportation conditions.

3. In-situ Load Tests

The instruments and equipment adopted for the field bearing plate creep tests are as follows: hydraulic jacks, hydraulic cushions, load cells, hydraulic pumps, hydraulic pipelines, pressure gauges, pressure stabilizing devices, circular rigid bearing plates, grating displacement sensors, reaction devices, constant temperature and humidity devices, temperature and humidity control systems, data acquisition systems, and monitoring systems [14] [15] [16] [17].

The field rock creep tests in this study were carried out by means of the surcharge loading method (as shown in Figure 2), using a self-developed intelligent rock rheology control system integrated with an intelligent temperature and humidity regulation system, automatic data acquisition module and remote monitoring module. The field creep tests were performed with the bearing plate method, in accordance with the Specifications for Rock Tests in Water Resources and Hydropower Engineering (SL/T 264-2020) and the Standard Methods for Engineering Rock Mass Testing (GB/T 50266-2013). The objectives of the tests are to provide a theoretical basis for the long-term stability of the foundation and offer reference data for the comparative verification of laboratory test results [19] [20] [21].

Given that the foundation pressure of the power plant generally ranges from 600 kPa to 800 kPa, and the maximum foundation pressure of the main plant may reach 1.1 MPa, the maximum pressure designed for the tests should be no less than 1.3 MPa. For stepwise incremental loading or stepwise incremental cyclic loading, the number of load steps should not be less than three, and the test load at each step is preferably graded at equal intervals. In this study, four load steps were designed with a maximum applied pressure of 2.0 MPa, which were divided into three graded levels of 0.5 MPa, 0.9 MPa and 1.3 MPa.

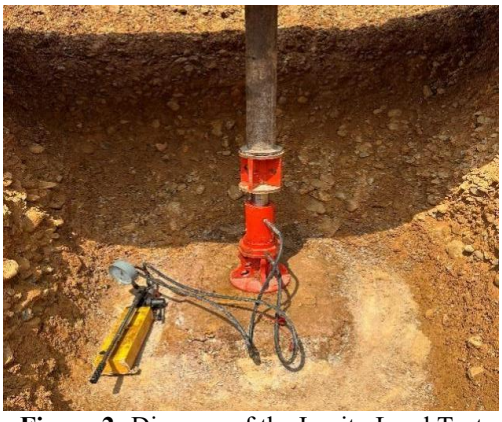

Figure 2: Diagram of the In-situ Load Test

4. Test Results and Analysis

4.1 Creep Test Data

The creep test results were obtained via the stepwise loading method. Considering the discreteness of the mechanical properties of the specimens from the target stratum, the stepwise loading method was adopted for the field in-situ creep tests, and the linear superposition method was employed for data processing.

Table 1: In-situ Test Data Sheet (After Linear Superposition)

0.5 MPa		0.9 MPa		1.3 MPa	
Time (h)	Displacement (mm)	Time (h)	Displacement (mm)	Time (h)	Displacement (mm)
0	0.783	0	1.145	0	1.477
0.017	0.791	0.017	1.161	0.017	1.499
0.034	0.803	0.034	1.188	0.034	1.542
0.051	0.813	0.051	1.213	0.051	1.582
0.068	0.819	0.068	1.232	0.068	1.616
0.083	0.824	0.083	1.25	0.083	1.646
0.118	0.826	0.118	1.263	0.118	1.673
0.167	0.829	0.167	1.276	0.167	1.697
0.25	0.831	0.25	1.287	0.25	1.719
0.334	0.834	0.334	1.299	0.334	1.742
0.417	0.837	0.417	1.311	0.417	1.763
0.5	0.839	0.5	1.32	0.5	1.781
0.583	0.841	0.583	1.33	0.583	1.799
0.75	0.846	0.75	1.341	0.75	1.818
1	0.849	1	1.351	1	1.835
2	0.858	2	1.366	2	1.857
3	0.864	3	1.378	3	1.875
4	0.869	4	1.388	4	1.891
5	0.874	5	1.398	5	1.906
6	0.877	6	1.406	6	1.919
7	0.878	7	1.411	7	1.928
9	0.882	9	1.419	9	1.941
11	0.885	11	1.426	11	1.952
13	0.886	13	1.43	13	1.96
15	0.886	15	1.433	15	1.966
17	0.886	17	1.436	17	1.973
20	0.886	20	1.437	20	1.977
24	0.887	24	1.439	24	1.98
26	0.887	26	1.44	26	1.983
34	0.887	34	1.441	34	1.985
40	0.887	40	1.441	40	1.985
48	0.887	48	1.441	48	1.985
56	0.887	58	1.441	58	1.986
64	0.887	70	1.441	70	1.986
72	0.887	84	1.442	84	1.987
		100	1.442	100	1.988
		118	1.442	118	1.988
		138	1.442	138	1.988
				160	1.988

The displacement-time curves under different loads were obtained by processing the stepwise loading data with the linear superposition method (Figure 3). The curves show that with the increase of load, the creep deformation increases, and the steady-state creep stage appears under high loads.

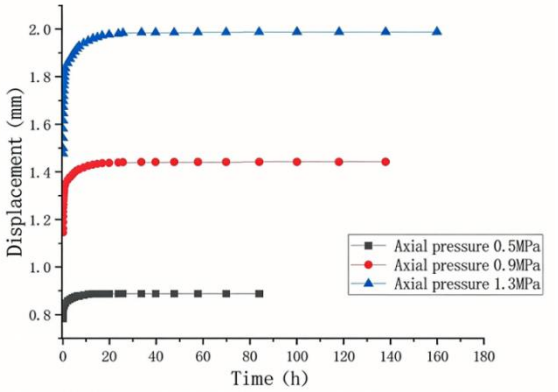

Figure 3: Creep Curves After Linear Superposition

4.2 Establishment and Parameter Fitting of the Burgers Creep Model

4.2.1 Creep Constitutive Model for In-situ Tests

The nonlinear viscoelastic rheological model of rock reflects the properties of linear viscoelastoplastic materials by means of some basic components, such as springs, dashpots, and plastic elements. These basic components are connected in parallel or series to form a nonlinear rheological constitutive model. The Burgers body is an elastoviscous body, which is composed of a Maxwell body and a Kelvin body connected in series. Its constitutive equations are shown in Equations (1) and (2).

$$\frac{\eta}{E_0}\dot{\sigma} + \left(1 + \frac{E_1}{E_0}\right)\sigma = \eta\dot{\varepsilon} + E_1\varepsilon \tag{1}$$

$$\ddot{\sigma} + \left(\frac{E_1}{\eta_2} + \frac{E_1}{\eta_1} + \frac{E_0}{\eta_2}\right)\dot{\sigma} + \frac{E_1E_0}{\eta_1\eta_2}\sigma = E_1\ddot{\varepsilon} + \frac{E_1E_0}{\eta_2}\dot{\varepsilon} \tag{2}$$

The Burgers model exhibits the properties of instantaneous elastic deformation, decelerated creep, and steady-state creep, and it is quite applicable to soft rocks (e.g., argillaceous rocks).

It is known that the compressive deformation of the rock mass surface at the edge of the rigid bearing plate is expressed as follows:

$$\overline{w}(s) = A\frac{1-\overline{\mu}(s)^2}{s\overline{E}(s)} \tag{3}$$

For the Burgers model, the compressive deformation of the rock mass surface in the Laplace domain is expressed as follows:

$$\overline{W}(s) = \frac{A}{4}\frac{1+\left(\frac{\eta_1}{G_0}+\frac{\eta_1+\eta_2}{G_1}\right)s+\frac{\eta_1\eta_2}{G_0G_1}s^2}{s^2\left(\eta_2+\frac{\eta_1\eta_2}{G_1}\right)s}\left[1+\frac{3\left(\eta_2+\frac{\eta_1\eta_2}{G_1}\right)s}{3K+\left[3K\left(\frac{\eta_2}{G_0}+\frac{\eta_1+\eta_2}{G_1}+\eta_2\right)\right]s+\left(3K\frac{\eta_1\eta_2}{G_0G_1}+\frac{\eta_1\eta_2}{G_1}\right)}\right] \tag{4}$$

Perform the inverse Laplace transform on Equation (4), and the final expression for the compressive deformation of the rock mass surface at an arbitrary time is obtained as follows:

$$w(t) = \frac{\pi pR_0}{8}\left[\frac{1}{K} + \frac{t}{\eta_2} + \left(\frac{1}{G_0}+\frac{1}{G_1}\right)\left(1-e^{\frac{G_1}{\eta_1}t}\right) - \frac{1}{G_0}e^{\frac{G_1}{\eta_1}t} - \frac{\eta_2\left(e^{-a_1t}-e^{-a_2t}\right)+\frac{\eta_1\eta_2}{G_1}\left(a_2e^{-a_1t}-a_1e^{-a_2t}\right)}{K\left(3K\frac{\eta_1\eta_2}{G_0G_1}+\frac{\eta_1\eta_2}{G_1}\right)(a_2-a_1)}\right] \tag{5}$$

Where

$$a_{1,2} = \frac{\left(3K\left(\frac{\eta_2}{G_0}+\frac{\eta_1+\eta_2}{G_1}+\eta_2\right)\pm\sqrt{\left(3K\left(\frac{\eta_2}{G_0}+\frac{\eta_1+\eta_2}{G_1}\right)+\eta_2\right)^2-12K\left(3K\frac{\eta_1\eta_2}{G_0G_1}+\frac{\eta_1\eta_2}{G_1}\right)}\right)}{2\left(3K\frac{\eta_1\eta_2}{G_0G_1}+\frac{\eta_1\eta_2}{G_1}\right)} \tag{6}$$

η_1 and η_2 are viscosity coefficients.

4.2.2 Parameter Identification of the In-situ Creep Model

1) Identification of Elastic Parameters

A certain abrupt displacement occurs on the surface of the rock mass when loading or unloading starts in the in-situ rheological test, which is usually referred to as instantaneous elastic deformation. Based on the formula for instantaneous elastic deformation of the rock mass surface at the edge of the rigid bearing plate, the instantaneous deformation modulus E0 of the rock mass under compressive load can be derived as follows:

$$E_0 = (1-\mu^2)\frac{\pi p}{2w}R_0 \tag{7}$$

Wherein, p denotes the stepwise compressive load, in MPa; w represents the abrupt displacement value of the rock mass, in cm; R_0 is the radius of the rigid bearing plate, in cm; μ stands for Poisson's ratio.

The calculation formulas for its shear modulus and bulk modulus are expressed as follows:

$$G_0 = \frac{E_0}{2(1+\mu)}, K = \frac{E_0}{3(1-2\mu)} \tag{8}$$

Table 2: Calculation Results of Elastic Parameters from Field Creep Tests

P(MPa)	E_0(MPa)	G_0(MPa)	K(MPa)
0.5	228.0815	87.7237	190.0679
0.9	280.7489	107.9803	233.9574
1.3	314.3720	120.9123	261.9767

2) Identification of Viscosity Parameters

The curves of the in-situ creep load tests indicate that under different load levels, the surface displacement of the rock mass develops with time. At relatively low loads, the creep deformation gradually attenuates until reaching a final stable state. With the increase of load magnitude, the creep deformation increases, and the rock mass exhibits distinct steady-state creep characteristics.

According to the theory of viscoelasticity, the mudstone at the test site is a typical viscoelastic material with both elastic deformation and viscous deformation characteristics. Based on the results of the field compressive creep tests, the least squares method was adopted for the fitting analysis of the rheological curves via numerical analysis.

According to the derived expressions of the Burgers model for field compressive rheology under the rigid bearing plate, the field compressive rheological test curves were fitted using custom-built fitting formulas. The fitting results are shown in Figs. 4 to 6, and the fitted results of the rheological model parameters are presented in Table 2.

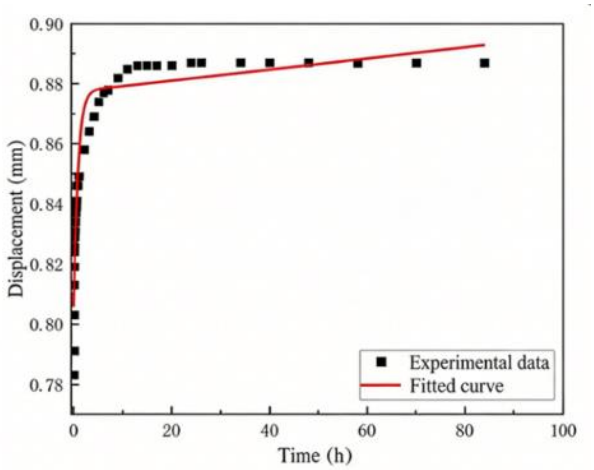

Figure 4: Fitting Curve Under 0.5 MPa Axial Compression

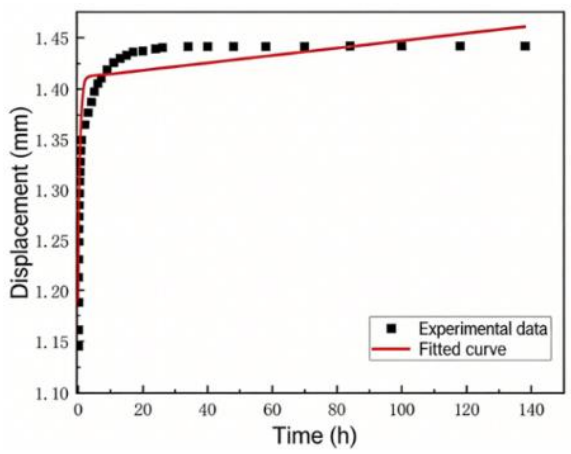

Figure 5: Fitting Curve Under 0.9 MPa Axial Compression

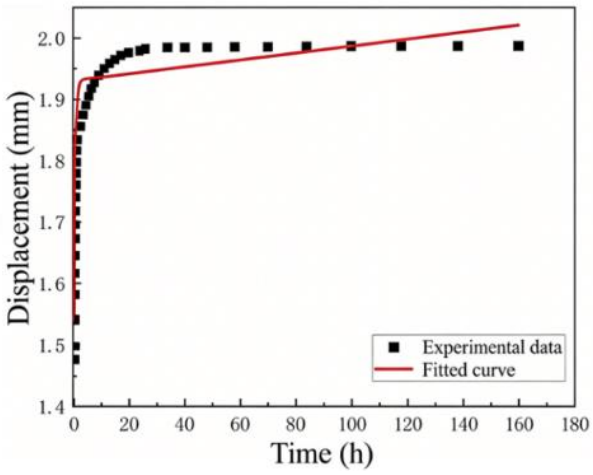

Figure 6: Fitting Curve Under 1.3 MPa Axial Compression

Table 3: Parameters and Fitting Results of Field In-situ Creep Tests

P(MPa)	G_1(MPa)	η_1(MPa·h)	η_2(MPa·h)	Fitting Results
0.5	6.208	5.6853	7320.7645	94.18%
0.9	7.579	2.1108	6536.7369	95.28%
1.3	8.450	1.6187	5359.4959	95.66%

The fitting results show that the goodness of fit of the model is all above 94%, indicating that the Burgers model can well describe the creep characteristics of the soft rock.

5. Discussion and Recommendations

This study systematically analyzed the creep mechanical properties of the soft rock in the foundation of a power plant via field in-situ load tests, established a Burgers creep constitutive model suitable for the specific geological conditions, and conducted an in-depth discussion on the applicability and engineering significance of the model.

1) The creep behavior of the soft rock exhibits significant load dependence. The in-situ test results show that under a relatively low load of 0.5 MPa, the rock mass deformation basically stabilizes after approximately 40 hours, showing typical attenuation creep characteristics. In contrast, when the load increases to 1.3 MPa, the deformation continues to develop for more than 160 hours, showing a tendency of approximate steady-state creep. This phenomenon reveals that the soft rock is dominated by structural compression and pore adjustment under low-stress conditions, whereas under high-stress conditions, intergranular slip and continuous propagation of microcracks may be activated, laying hidden dangers for its long-term deformation.

2) The successful application of the Burgers creep model is the key finding of this study. The results of model parameter identification indicate that the elastic modulus E0 increases from 228.08 MPa to 314.37 MPa with the increase of load, reflecting the compaction and hardening effects of the rock mass during stepwise loading. In contrast, the viscosity coefficient η2 decreases from 7320.76 MPa·h to 5359.50 MPa·h, which indicates that with the increase of stress level, the long-term flow deformation capacity of the rock mass is significantly enhanced, making it easier to enter the steady-state creep stage. The goodness of fit of all fitting curves exceeds 94%, demonstrating that this model can well characterize the entire process of soft rock deformation from instantaneous elastic deformation to viscous flow, and is particularly suitable for describing the rheological properties of weak rock masses such as sandy rocks.

3) The Burgers model and related parameters established in this study provide a quantitative tool for the evaluation of long-term engineering stability. By fitting the creep curves under different load levels, rheological parameters with clear physical meanings were obtained, which can be directly applied to numerical simulation analysis. In practical engineering, appropriate model parameters can be selected according to the actual stress state of the foundation for long-term deformation prediction. In particular, when the load level exceeds 1.0 MPa, the rock mass shows an obvious steady-state creep tendency. This suggests that special attention should be paid to the long-term stability of high-stress areas during the engineering design stage, and pre-reinforcement measures should be taken if necessary.

References

[1] Zhang Z, Ruan C, Liu Z. Two improved physics-informed Neural Networks for solving Burgers equation [J]. Journal of Computational Science, 2026, 93102756-102756.DOI:10.1016/J.JOCS.2025.102756.

[2] Kumar D, Pandit S. An efficient B-spline wavelet algorithm for simulation of viscous Burgers' and coupled Burgers' equations [J]. Computational and Applied Mathematics, 2025, 45(2): 55-55. DOI:10.1007/S40314-025-03437-Y.

[3] Wang H,Zheng W,Shao L, et al. Creep characteristics and constitutive model construction of offshore soft soils [J]. Journal of Traffic and Transportation Engineering (English Edition), 2025, 12(5): 1360-1374. DOI:10.1016/J.JTTE.2022.12.004.

[4] Salama M F. An efficient explicit group method for time fractional Burgers equation [J]. Frontiers in Physics, 2025, 131631259-1631259. DOI:10.3389/FPHY.2025.1631259.

[5] Ueda Y. Linear stability of the non-zero equilibrium state for the viscous Burgers equation with time delay [J]. Japan Journal of Industrial and Applied Mathematics, 2025,42(5):1-16.DOI:10.1007/S13160-025-00706-5.

[6] Yan Y, Chang D, Liu J, et al. Triaxial creep tests and DEM simulation of frozen clay incorporating the

Burgers model [J]. Cold Regions Science and Technology,2025,237104519-104519.DOI:10.1016/J.COLDREGIONS.2025.104519.
[7] Shu X, Chen W, Tian H, et al. Resilience analysis of tunnel lining under creep-induced convergence of soft rock: Characterization and field application [J]. Tunnelling and Underground Space Technology incorporating Trenchless Technology Research, 2025, 163106691-106691.DOI:10.1016/J.TUST.2025.106691.
[8] Huang J, Hu S, Li X, et al. Creep Model of Weakly Cemented Soft Rock Considering Damage and Secondary Development in FLAC3D [J]. Applied Sciences,2025,15(9):4838-4838.DOI:10.3390/APP15094838.
[9] Liu J, Zhou N, Zhou H, et al. Creep Damage Characteristics and Fractional-Order Model of Weakly Cemented Soft Rock [J]. Rock Mechanics and Rock Engineering,2025,58(7):1-21.DOI:10.1007/S00603-025-04539-Z.
[10] Wenkai R, Shanchao H, Aohui Z, et al. Study on Creep Characteristics and Nonlinear Fractional-Order Damage Constitutive Model of Weakly Cemented Soft Rock [J]. Rock Mechanics and Rock Engineering, 2023, 56(11): 8061-8082.DOI:10.1007/S00603-023-03493-Y.
[11] Zhou C, Yu L, You F, et al. Coupled Seepage and Stress Model and Experiment Verification for Creep Behavior of Soft Rock [J]. International Journal of Geomechanics, 2020,20(9):04020146-04020146.DOI:10.1061/(ASCE)GM.1943-5622.0001774.
[12] Huang M, Zhan W J, Xu S C, et al. New Creep Constitutive Model for Soft Rocks and Its Application in the Prediction of Time-Dependent Deformation in Tunnels [J]. International Journal of Geomechanics, 2020, 20(7): 04020096-04020096. DOI:10.1061/(ASCE)GM.1943-5622.0001663.
[13] ŽIVALJEVIĆ S, TOMANOVIĆ Z, MILADINOVIĆ B. Creep behaviour of a layered soft rock around the tunnel opening [J]. ce/papers, 2018, 2(2-3): 1057-1062. DOI:10.1002/cepa.812.
[14] Guo Z M,Yan Y W. A Study of Creep Similarity Criterion of Soft Rock in Temperature-Stress Environment [J]. Key Engineering Materials, 2016, 717(717-717):136-139.DOI:10.4028/WWW.SCIENTIFIC.NET/KEM.717.136.
[15] Zvonko T. Testing of creep phenomena on soft rock [J]. Gradjevinski materijali i konstrukcije, 2014, 57(3): 21-41. DOI:10.5937/grmk1403021t.
[16] Wang Y Y, Li F, Tai J X. Experimental Investigating of Latex Cement as Similar Material Simulating Soft Rock Creep [J].Advanced Materials Research, 2012, 1896(535-537):1940-1943.DOI:10.4028/www.scientific.net/AMR.535-537.1940.
[17] Zhiliang F, Hua G, Yanfa G. Creep Damage Characteristics of Soft Rock under Disturbance Loads [J]. Journal of China University of Geosciences, 2008, 19(3): 292-297.DOI:10.1016/S1002-0705(08)60047-3.
[18] Zhiliang F, Hua G, Yanfa G A. Experimental Study on CT Micro Mechanics Characteristics of Soft Rock Creep under Gravity Disturbance Loads [J]. International Conference on Computational & Experimental Engineering and Sciences, 2008, 5(3): 145-156. DOI:10.3970/icces.2008.005.145.
[19] Tomanovic Z. Rheological model of soft rock creep based on the tests on marl [J]. Mechanics of time-dependent materials, 2006, 10(2): 135-154. DOI:10.1007/s11043-006-9005-2.
[20] MA Y, ZHANG Y. Experimental Research on Creep and Hydrate Laws of Heterogeneous Soft Rock under Deep Mining [C],2011:
[21] Chun L, Heng L, Haizhuang L, et al. Study on Creep Test and Constitutive Model of Layered Soft Rock [C], 2023: DOI:10.2991/978-94-6463-336-8_8.